

# Precision Measurement of Boron to Carbon flux ratio in Cosmic Rays from 2 GV to 1.8 TV with the Alpha Magnetic Spectrometer on the International Space Station.

---

**A. Oliva\* on behalf of the AMS Collaboration<sup>†</sup>**

*Centro de Investigaciones Energéticas, Medioambientales y Tecnológicas, CIEMAT, E-28040 Madrid, Spain.*

*E-mail: [alberto.oliva@cern.ch](mailto:alberto.oliva@cern.ch)*

AMS-02 is wide acceptance high-energy physics experiment installed on the International Space Station in May 2011 and operating continuously since then. AMS-02 is able to precisely separate cosmic rays light nuclei ( $1 \leq Z \leq 8$ ) with contaminations less than  $10^{-3}$ . The light nuclei cosmic ray Boron to Carbon flux ratio is very well known sensitive observable for the understanding of the propagation of cosmic rays in the Galaxy, being Boron a secondary product of spallation on the interstellar medium of heavier primary elements such as Carbon and Oxygen. A precision measurement based on 10 million events of the Boron to Carbon ratio in the rigidity range from 2 GV to 1.8 TV is presented.

*The 34th International Cosmic Ray Conference,  
30 July- 6 August, 2015  
The Hague, The Netherlands*

---

\*Speaker.

<sup>†</sup>for the complete list of authors see the AMS Collaboration list in these proceedings.

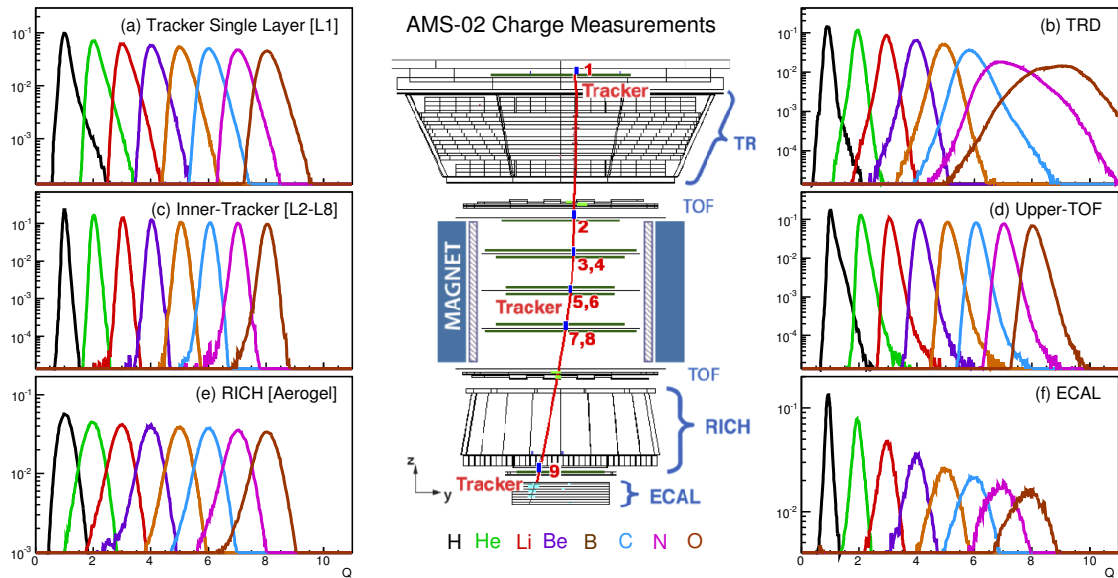


**Figure 1:** A charged particle traversing AMS-02 is depicted in the center of the figure. The absolute charge  $|Z|$  of the particle is measured several times along the particle trajectory. From the top to the bottom of the detector charge estimators are given by: Tracker L1, TRD, Upper TOF, Inner Tracker, Lower TOF, RICH, Tracker L9, and ECAL. On the left and on the right the charge distributions of the listed measurements are presented for clean samples of ions with  $1 \leq |Z| \leq 8$ .

## 1. Introduction

Boron is originated by reactions of heavier elements on the interstellar medium such as Carbon and Oxygen. The Boron to Carbon ratio is a direct probe of the mechanisms that rule propagation of cosmic rays in the Galaxy [1]. It is also a convenient quantity to be measured by experimentalists since Boron and Carbon are neighbouring elements in the table of elements and have similar interactions in matter. Measurements from the seventies up to today are available in the following Ref. [2][3][4][5][6][7][8][9][10][11][12][13].

AMS-02 is a general purpose high energy magnetic spectrometer in space. The design of the AMS-02 detector is described in detail in Ref. [14]. It consists of nine planes of precision Silicon Tracker, a transition radiation detector (TRD), four planes of time-of-flight counters (TOF), a permanent magnet, an array of anti-coincidence counters (ACC) surrounding the inner tracker, a ring imaging Čerenkov detector (RICH), and an electromagnetic calorimeter (ECAL).

Charge of the particle is measured several times along the particle trajectory: on top of AMS by a layer of Silicon sensors constituting the Tracker L1; in the TRD by the combination of measurements in the 20 layers of straw tubes; in the Inner Tracker by the combination of 7 single layer Tracker measurements (from L2 to L8); in the Upper TOF (UTOF) by the combination of the measurements of two layers of scintillating counters; on the Lower TOF (LTOF) similarly to UTOF; in the RICH by counting the number of photons emitted by the Čerenkov emission; on the Tracker L9; and by the the energy deposit measurement in the first layers of ECAL that show no inelastic interaction. In Fig. 1 the charge distribution of the multiple AMS charge estimators are presented.

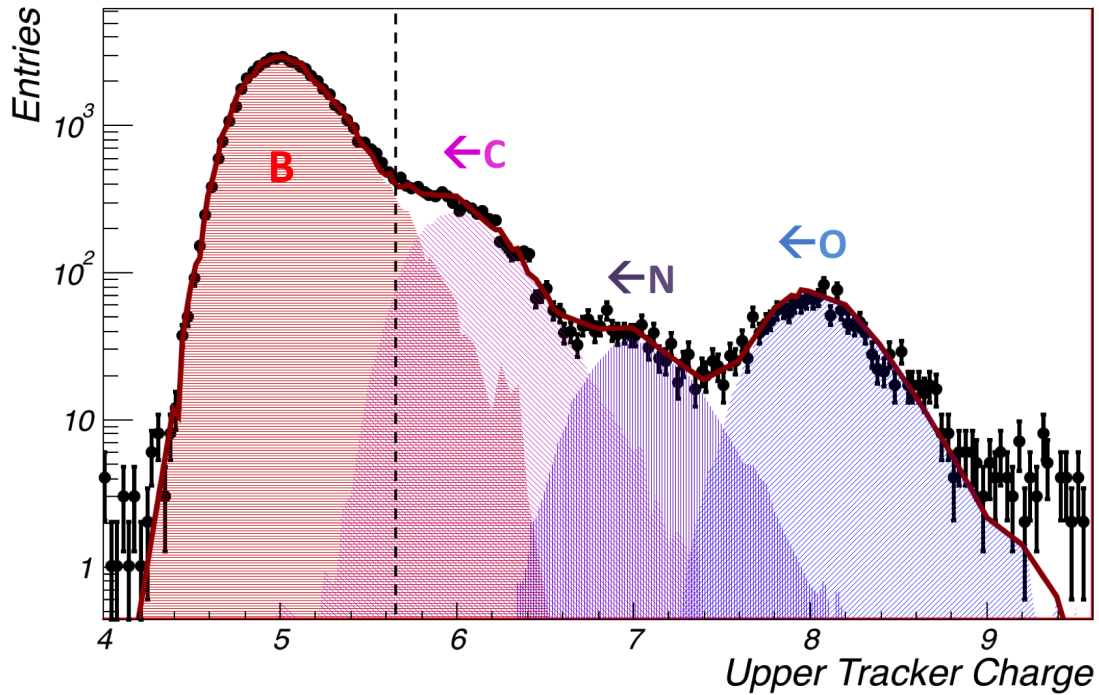


**Figure 2:** Charge of the Tracker L1 for a low contamination Boron sample selected with in the Inner Tracker. The charge distribution shows a large population of not-interacting Boron events, as well as a population of higher  $Z$  nuclei (C, N, O) that interacted in the upper part of AMS giving emerging B fragments. Using the knowledge of the spectral shape of charge on L1 and using simple cuts is possible to select samples with contaminations less than 3% and selection efficiencies  $> 95\%$  at all energies.

Best responses are given by the Inner Tracker, UTOF and LTOF with resolutions of  $\Delta Z = 0.12$ , 0.16 and 0.16 respectively for  $Z = 6$ .

Measurement of particle rigidity is derived by the measurement of the particle curvature in the magnetic field. The nine position measurements along the particle trajectory on a lever arm of about 3 meters between L1 and L9 give a Maximum Detectable Rigidity (that is, the rigidity for which  $\Delta R/R = 1$ ) of about 2.5 TV for  $Z = 6$ .

Monte Carlo simulated events were produced using a dedicated program developed by the collaboration based on the GEANT-4.10.1 package [17], where nucleus-nucleus interactions were modelled with the DPMJET-II.5 package [18] above, and the Binary Light Ion Cascade model [17] for energy below 5 GeV/nucleon. The program simulates transport of ions through AMS materials. Digitization of the signals is simulated precisely according to the measured characteristics of the electronics.

The use of Monte Carlo in this analysis is limited to the estimation of geometric acceptances, evaluation of the response function of the Tracker, and the top-of-the-instrument correction.

## 2. Selection

Data collected in the first 40 months of AMS operation have been analysed. Downward going

particles with charge 5 and 6 in the Inner Tracker and UTOF are firstly selected. The efficiency of this selection is very high, up to 98% with a negligible probability of assigning a particle a wrong charge. To control interaction in the detector only events that have a charge measurement on Tracker L1 are used in the analysis. In order to have the best resolution at the highest rigidities, further selections are made by requiring track fitting quality criteria such as minimum request on  $\chi^2/d.f.$  in the bending coordinate. To select only primary cosmic rays the measured rigidity is required to be greater than a factor of 1.2 times the maximum geomagnetic cutoff within the AMS field of view. The cutoff was calculated by backtracing [15] particles from the top of AMS out to 50 Earth's radii using the most recent IGRF [16] geomagnetic model. The final sample consists in about  $7 \times 10^6$  Carbons and  $2 \times 10^6$  Boron.

These events are then used for 2 different analysis. An analysis that require the presence of charge measurement compatible with  $Z = 5, 6$  on Tracker L9, and an analysis that does not have any additional request on the lower part of AMS. The first analysis has the largest level arm and exploits the best rigidity resolution, the second analysis instead has a much larger statistics and lower interaction levels inside the detector. The two analysis have been found to be compatible and combined in the final B/C ratio to have, whenever possible, maximum statistics and best rigidity resolution.

Nuclei may interact on AMS materials and split into fragments of lower charge. In Fig. 2 is presented the charge distribution on top of AMS measured by L1 for a clean selection of Boron with UTOF and Inner Tracker. The population of Carbons, Nitrogens and Oxygens correspond to the charge-changing processes  $O \rightarrow B$ ,  $N \rightarrow B$  and  $C \rightarrow B$  happening between L1 and UTOF. To estimate the purity of the sample on L1 a fitting procedure has been developed. Reference spectra for each charge were derived and used to fit the distribution obtained after cuts, as presented in Fig. 2. Purity of the Boron sample is  $> 97\%$  with an efficiency of  $\sim 96\%$ . Carbon purity and efficiency are instead very close to 1, since the large abundance of Carbon allows selections of high efficiency and tiny backgrounds.

Charge-changing process happening in materials above L1 are taken into account into the counts calculation. This determination relies in the MC simulation of materials in front of L1, essentially constituted by supporting structures. The most significant interaction channel is about 0.5% of cosmic ray Carbon flux undergoing a charge change interaction above the L1 and giving Boron fragments reconstructed as a good Boron events from our selection. This contribution, as well the similar one derived from Oxygen, is subtracted from the Boron counts.

The rigidity bin-to-bin migration of events was corrected using the iterative unfolding procedure described in Ref. [19].

### 3. Analysis and result

The Boron-to-Carbon ratio can be written as a ratio of two isotropic flux  $\Phi_i^Z$  for the  $i^{\text{th}}$  rigidity bin  $(R_i, R_i + \Delta R_i)$  as:

$$\Phi_i^Z = \frac{N_i^Z}{A_i^Z \varepsilon_i^Z T_i \Delta R_i} \quad \rightarrow \quad B/C = \frac{\Phi_i^B}{\Phi_i^C} = \frac{N_i^B}{N_i^C} \cdot \left[ \frac{A_i^B}{A_i^C} \cdot \frac{\varepsilon_i^B}{\varepsilon_i^C} \right]^{-1} \quad (3.1)$$

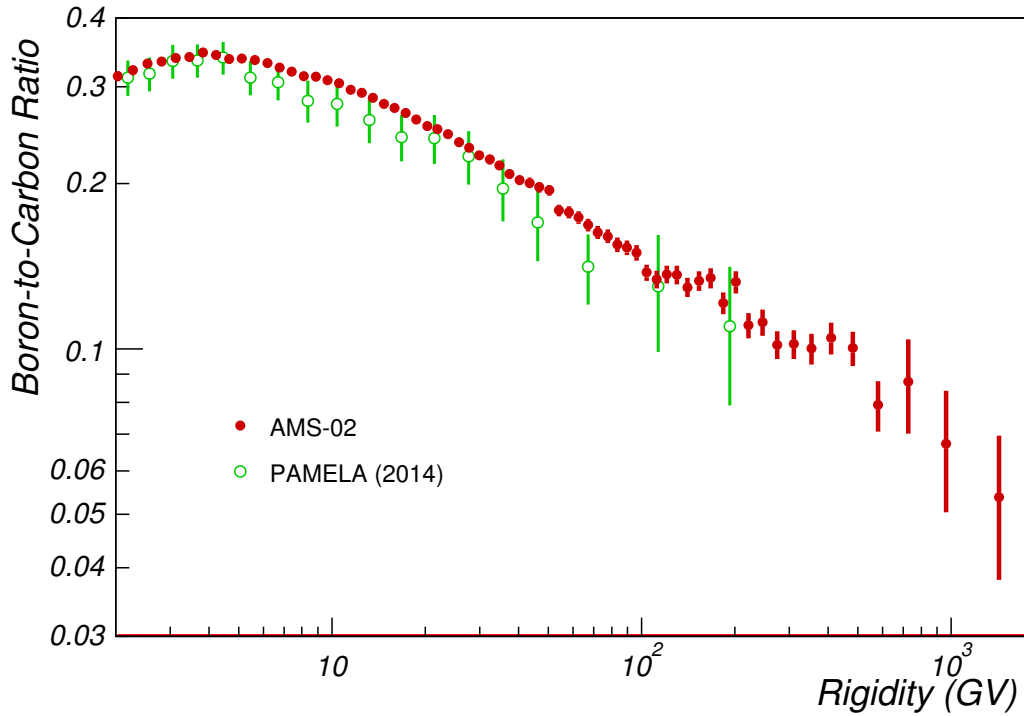


**Figure 3:** The derived Boron-to-Carbon ratio in rigidity units. Measurement of PAMELA [13] is shown for comparison.

where  $N_i^Z$  are the number of events corrected for charge migrations inside the detector, for charge migration above L1 and for the rigidity resolution function.  $A_i^Z$  is the geometric acceptance evaluated in MC,  $\varepsilon_i^Z$  is the byproduct of efficiencies estimated directly from data,  $T_i$  is the collection time. In the B/C ratios of efficiency terms tends to cancel out since interaction in matter of Boron and Carbon are similar. Ratio of efficiencies estimated directly from data include trigger efficiency, TOF efficiency, tracking efficiency, efficiency in finding external hits. The survival probability of Boron and Carbon interacting in the lowest part of AMS, representing about 1/3 of AMS materials, has been calculated and used to account for the difference of inelastic interaction of B and C in matter.

The derived B/C ratio in the rigidity range between 2 GV to 1.8 TV is presented in Fig. 3 compared with recent publication in rigidity Ref. [13]. Errors include statistics that is dominating error after 50 GV, and systematics due to charge migration inside AMS, charge migration above L1, rigidity migration, efficiency and acceptance ratio corrections.

To compare with previous result, published mostly in kinetic energy per nucleon, we converted our rigidity measurement into kinetic energy. Single rates of B and C in rigidity are firstly calculated, then converted into kinetic energy following different  $A/Z$  hypothesis for the different isotopes. Then spectra are summed using as weight the isotopic composition and corrected for efficiency ratios. Carbon has been assumed to be purely composed by  $^{12}\text{C}$  and Boron to have a relative abundance of  $^{11}\text{B}/(^{10}\text{B}+^{11}\text{B}) = 0.7$ . A 0.1 error on Boron composition has been considered as sys-

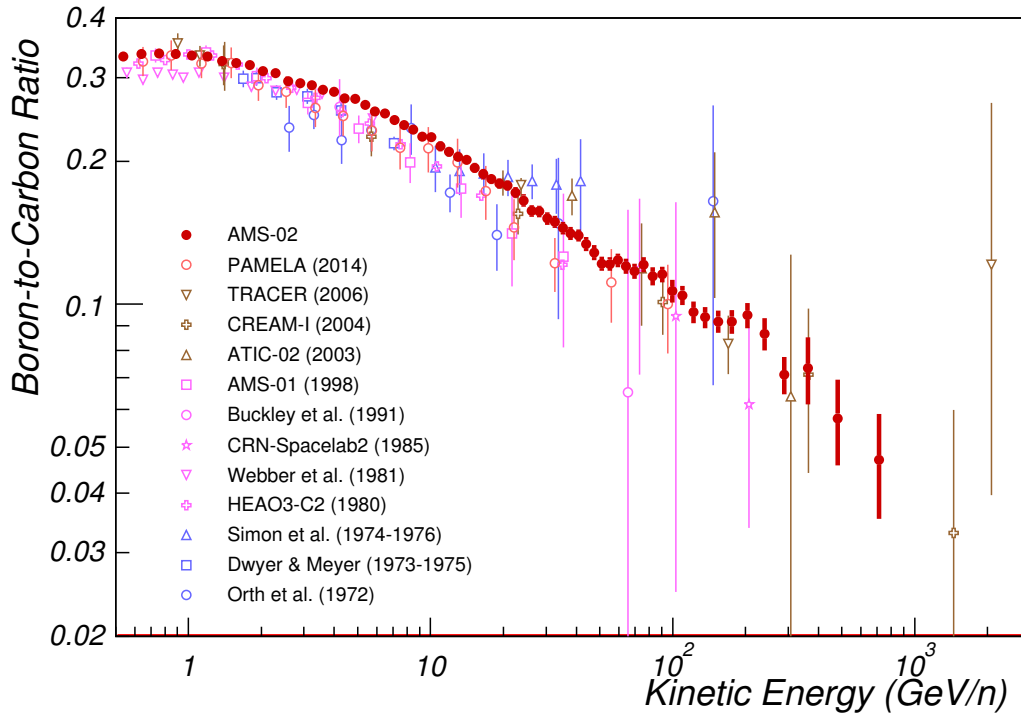


**Figure 4:** The derived Boron-to-Carbon ratio. Available B/C measurements in the range from 0.5 to 700 GeV/n are shown for comparison: Orth et al. [2], Dwyer and Meyer [3], Simon et al. [4], HEAO3-C2 [5], Webber et al., [6], CRN-Spacelab2 [7], Buckley et al. [8], AMS-01 [9], ATIC-02 [10], CREAM-I [11], TRACER [12] and PAMELA [13].

tematic error. This translates into a up to 3 % additional systematic error on the Boron-to-Carbon ratio. In Fig. 4 the derived B/C ratio in kinetic energy per nucleon is shown.

#### 4. Conclusions

The light nuclei cosmic ray Boron to Carbon flux ratio is very well known sensitive observable for the understanding of the propagation of cosmic rays in the Galaxy, being Boron a secondary product of spallation on the interstellar medium of heavier primary elements such as Carbon and Oxygen. A precision measurement based on 10 million events of the Boron to Carbon ratio in the rigidity range from 2 GV to 1.8 TV has been presented.

#### References

- [1] A. W. Strong, I. V. Moskalenko, and V. S. Ptuskin, *Annual Rev. of Nucl. and Part. Science* **57**, 285 (2007).
- [2] C.D. Orth *et al.*, *Astrophys. J.* **226**, 1147 (1978).
- [3] R. Dwyer and P. Meyer, *Astrophys. J.* **322**, 981 (1987).
- [4] M. Simon *et al.*, *Astrophys. J.* **239**, 712 (1980).

- [5] J.J. Engelmann *et al.*, *Astron. Astrophys.* **233**, 96 (1990).
- [6] W. R. Webber *et al.*, *Proceedings of 19th Intern. Cosmic Ray Conf. La Jolla*, **2**, 16 (1985).
- [7] D. Muller *et al.*, *Astrophys. J.* **374**, 356 (1991).
- [8] J. Buckley *et al.*, *Astrophys. J.* **429**, 736 (1994).
- [9] M. Aguilar *et al.*, *Astrophys. J.* **724**, 328 (2010).
- [10] A.D. Panov *et al.*, *Proceedings of the 23rd Intern. Cosmic Ray Conf.*, Mérida, **2**, 3 (2008).
- [11] H.S. Ahn *et al.*, *Astropart. Phys.* **30**, 133 (2008).
- [12] A. Obermeier *et al.*, *Astrophys. J.* **752**, 69 (2012).
- [13] O. Adriani *et al.*, *Astrophys. J.* **791**, 93 (2014).
- [14] A. Kounine, *Int. J. Mod. Phys. E* **21** 1230005 (2012).
- [15] J. Alcaraz *et al.*, *Phys. Lett. B* **484**, 10 (2000);
- [16] C. C. Finlay *et al.*, *Geophys. J. Int.* **183/3**, 1216 (2010). We have used data from IGRF-12 (2015), currently available at <http://www.ngdc.noaa.gov/IAGA/vmod/igrf.html> (unpublished).
- [17] S. Agostinelli *et al.*, *Nucl. Instrum. Methods Phys. Res., Sect. A* **506**, 250 (2003).
- [18] J. Ranft, *Phys. Rev. D* **51**, 64 (1995) .
- [19] M. Aguilar *et al.*, *Phys. Rev. Lett.* **114** , 171103(2015) ;